Experimental evidence for excess entropy discontinuities in glass-forming solutions

Daniel M. Lienhard, Bernhard Zobrist, Andreas Zuend, Ulrich K. Krieger, and Thomas Peter

Citation: J. Chem. Phys. **136**, 074515 (2012); doi: 10.1063/1.3685902
View online: http://dx.doi.org/10.1063/1.3685902
View Table of Contents: http://jcp.aip.org/resource/1/JCPSA6/v136/i7
Published by the American Institute of Physics.

Experimental evidence for excess entropy discontinuities in glass-forming solutions

Daniel M. Lienhard,[1,a)] Bernhard Zobrist,[1,2] Andreas Zuend,[3] Ulrich K. Krieger,[1] and Thomas Peter[1]

[1]*Institute for Atmospheric and Climate Science (IAC), ETH Zurich, Switzerland*
[2]*Faculty of Chemistry, Bielefeld University, Bielefeld, Germany*
[3]*Department of Chemical Engineering, California Institute of Technology, Pasadena, California 91125, USA*

(Received 20 September 2011; accepted 31 January 2012; published online 21 February 2012)

Glass transition temperatures T_g are investigated in aqueous binary and multi-component solutions consisting of citric acid, calcium nitrate ($Ca(NO_3)_2$), malonic acid, raffinose, and ammonium bisulfate (NH_4HSO_4) using a differential scanning calorimeter. Based on measured glass transition temperatures of binary aqueous mixtures and fitted binary coefficients, the T_g of multi-component systems can be predicted using mixing rules. However, the experimentally observed T_g in multi-component solutions show considerable deviations from two theoretical approaches considered. The deviations from these predictions are explained in terms of the molar excess mixing entropy difference between the supercooled liquid and glassy state at T_g. The multi-component mixtures involve contributions to these excess mixing entropies that the mixing rules do not take into account. © *2012 American Institute of Physics*. [http://dx.doi.org/10.1063/1.3685902]

I. INTRODUCTION

Glass formation can occur upon rapid cooling of liquids like polymer blends or aqueous solutions. The atoms or molecules in a glass move very slowly but are not fixed to regular lattice structures as in a crystal. Since this slow movement results in limited transport of momentum, a glass exhibits high viscosity and behaves mechanically like a solid.[1] The industrial applications of glasses range from window glasses to engineering plastics,[2] silicon and photovoltaic cells,[3] food technology[4] to pharmaceutical industries[5] and cryobiology.[6] Highly viscous liquids also play a major role in nature. Jenniskens and Blake[7] speculate that most of the water in the universe resides in the glassy state. Recently, Zobrist *et al.*[8] and Murray[9] suggested that organic dominated aerosol particles might turn glassy and exhibit high viscosity near the tropopause region. Organic aerosol particles are, among other emission sources, produced by biomass burning in the tropics[10,11] and they are ubiquitous in the troposphere (see Kanakidou *et al.*[12]). Murphy *et al.*[13] and Froyd *et al.*[14] detected particles that consist largely of organic material at the tropical tropopause level. The high viscosity of these particles could kinetically limit water uptake and thus inhibit the formation of cirrus clouds.[15–17] These limitations in water uptake could also explain the high supersaturations and impeded freezing of liquid droplets found by field studies[18–21] at these altitudes.

The competition between crystallization and glass formation upon cooling of a liquid determines whether a crystal forms or glass transition occurs.[22] Both the crystallization and glass formation depend on relaxation time which itself depends on the chemical and physical properties of the material.[6,23] When a liquid is cooled below its melting point T_m, crystallization might not take place immediately. It rather stays supercooled with respect to the crystalline state, usually referred to as metastable liquid. As an example, water can be supercooled to 235 K when no freezing-inducing surfaces are present, before ice formation occurs.[24] The contact-free crystallization temperature of aqueous solutions is often termed as the homogeneous ice freezing temperature, T_{hom}.

The glass formation is accompanied with a substantial reduction in the number of configurations that the system could adopt if it would remain liquid. This reduction reduces the entropy of the liquid and increases its viscosity. Therefore, the configurational entropy played an important role in the description of the glass transition temperature, T_g, and viscosity from theoretical considerations since the 1950s when Gibbs and co-workers established the theory of cooperative rearrangements.[25–27] Based on entropy concepts, Couchman and Karasz[28] derived an equation to compute T_g of a mixture of two components which depends solely on the properties of the pure components and the composition. Gordon and Taylor[29] published already earlier an equation of the same form to calculate the T_g of binary mixtures, which was derived from the additivity of specific volumes. In this work, we focus on the entropy based approach by Couchman and Karasz,[28] which is explained in detail in Sec. II.

We investigated the glass transition temperatures of complex aqueous mixtures using a differential scanning calorimeter (DSC) and used different approaches to model the experimental results. Solutions with both organic and inorganic constituents are investigated including citric acid, malonic acid, calcium nitrate ($Ca(NO_3)_2$), ammonium bisulfate (NH_4HSO_4), and raffinose whereas the solute weight fraction was varied between 0.111 and 0.851. The first four substances have been identified in atmospheric particles[10,11,30] and raffinose can be considered as a proxy for oxidized organic molecules with high molar masses.

a)Electronic mail: daniel.lienhard@env.ethz.ch.

II. THEORETICAL BACKGROUND

This section briefly explains the approach by Couchman and Karasz.[28] They expressed the molar entropy contribution of component i in an ideal liquid mixture S_i^{l} and in an ideal glassy mixture S_i^{g} at temperature T as[28,31]

$$S_i^{\mathrm{l}}(T) = \chi_i \left\{ S_i^0 + \int_{T_{\mathrm{g},i}}^{T} \frac{c_i^{\mathrm{l}}}{T'} \mathrm{d}T' \right\}, \tag{1}$$

$$S_i^{\mathrm{g}}(T) = \chi_i \left\{ S_i^0 + \int_{T_{\mathrm{g},i}}^{T} \frac{c_i^{\mathrm{g}}}{T'} \mathrm{d}T' \right\}. \tag{2}$$

χ_i denotes the mole fraction of component i in a mixture and S_i^0 its pure component molar entropy at $T_{\mathrm{g},i}$, i.e., the glass transition temperature of pure component i. c_i^{l} and c_i^{g} are the molar heat capacities of the pure component at constant pressure in the liquid and the glassy state, respectively. The total entropy of a non-ideal mixture can then be expressed as the sum of the ideal mixing entropies of the individual components plus an additional molar excess mixing entropy ΔS_{mix} accounting for non-ideal mixing.[28,32] Treating the glass transition as a second order phase transition, the sum of all entropy contributions of the glass and the liquid must be equal at the glass transition temperature of the mixture, i.e., at $T = T_{\mathrm{g}}$,

$$\sum_i S_i^{\mathrm{l}} + \Delta S_{\mathrm{mix}}^{\mathrm{l}} = \sum_i S_i^{\mathrm{g}} + \Delta S_{\mathrm{mix}}^{\mathrm{g}}. \tag{3}$$

$\Delta S_{\mathrm{mix}}^{\mathrm{l}}$ and $\Delta S_{\mathrm{mix}}^{\mathrm{g}}$ account for all deviations from ideal mixing of the components in the liquid and the glassy state, respectively.

From Eqs. (1)–(3), it follows that T_{g} can be expressed as[33]

$$T_{\mathrm{g}} = \exp\left\{ \frac{\sum_i \chi_i \left[c_i^{\mathrm{l}} - c_i^{\mathrm{g}}\right] \ln T_{\mathrm{g},i}}{\sum_i \chi_i \left[c_i^{\mathrm{l}} - c_i^{\mathrm{g}}\right]} - \frac{\Delta S_{\mathrm{mix}}^{\mathrm{l}} - \Delta S_{\mathrm{mix}}^{\mathrm{g}}}{\sum_i \chi_i \left[c_i^{\mathrm{l}} - c_i^{\mathrm{g}}\right]} \right\}. \tag{4}$$

Equation (4) can be simplified using the Taylor approximation, $\ln\left[1 + (T_{\mathrm{g},i} - T_{\mathrm{g}})/T_{\mathrm{g}}\right] \approx (T_{\mathrm{g},i} - T_{\mathrm{g}})/T_{\mathrm{g}}$. In this study, water is always used as solvent, i.e., substance 1. Expressed in weight fractions, this yields for an n-component system,

$$T_{\mathrm{g}} \cong \frac{w_1 T_{\mathrm{g},1} + \sum_{i=2}^{\mathrm{n}} w_i \frac{1}{k_i} T_{\mathrm{g},i}}{w_1 + \sum_{i=2}^{\mathrm{n}} w_i \frac{1}{k_i} + a\left(\Delta S_{\mathrm{mix}}^{\mathrm{l}} - \Delta S_{\mathrm{mix}}^{\mathrm{g}}\right)}, \tag{5}$$

with

$$k_i = \frac{\left[c_1^{\mathrm{l}} - c_1^{\mathrm{g}}\right] M_i}{\left[c_i^{\mathrm{l}} - c_i^{\mathrm{g}}\right] M_1}, \tag{6}$$

and

$$a = \frac{1}{c_1^{\mathrm{l}} - c_1^{\mathrm{g}}} \left\{ w_1 + \sum_{i=2}^{\mathrm{n}} w_i \frac{M_1}{M_i} \right\}. \tag{7}$$

M_1 and M_i are the molecular masses of water and solute i, w_1 and w_i denote their weight fractions, respectively. For a wide range of mixtures, the excess mixing entropy is assumed to not change significantly at T_{g}, thus Couchman and Karasz[28] assumed $\Delta S_{\mathrm{mix}}^{\mathrm{l}} - \Delta S_{\mathrm{mix}}^{\mathrm{g}} = 0$, which is used as a reference of an ideal vitrification. In addition, they assumed that the $c_i^{\mathrm{l}} - c_i^{\mathrm{g}}$'s are temperature independent as the mixture turns into a glass at a different temperature than the pure component. In these systems, T_{g} of a multi-component mixture can be computed when k_i and $T_{\mathrm{g},i}$ of all solutes are known,[34]

$$T_{\mathrm{g}} \cong \frac{w_1 T_{\mathrm{g},1} + \sum_{i=2}^{\mathrm{n}} w_i \frac{1}{k_i} T_{\mathrm{g},i}}{w_1 + \sum_{i=2}^{\mathrm{n}} w_i \frac{1}{k_i}}. \tag{8}$$

We refer to this equation as the Couchman–Karasz equation. In practise, k_i and $T_{\mathrm{g},i}$ are derived from data of the binary systems (see Sec. IV A).

For a binary mixture ($n = 2$), Eq. (8) reduces to

$$T_{\mathrm{g}} \cong \frac{w_1 T_{\mathrm{g},1} + w_2 \frac{1}{k_2} T_{\mathrm{g},2}}{w_1 + w_2 \frac{1}{k_2}}. \tag{9}$$

This equation coincides with the expression derived by Gordon and Taylor and others.[29,35] Different derivations of Eq. (9) are based on different physical interpretations of the parameters k_i. Since component 1 is water, the k_i's are parameters depending on the properties of solute i and water. As mentioned above, the heat capacities in Eqs. (1)–(7) denote the heat capacities of the pure components. The total difference of the heat capacity of the liquid and the glass measured at T_{g} in aqueous solutions will be called $c^{\mathrm{l}} - c^{\mathrm{g}}$, omitting the subscript.

III. EXPERIMENTAL

Glass transition temperatures, T_{g}, homogeneous ice freezing temperatures, T_{hom}, and ice melting temperatures, T_{m}, of different concentrated aqueous solutions (binary and multi-component mixtures consisting of inorganic and/or organic solutes, see Table III) were investigated in a differential scanning calorimeter (DSC, TA Instruments Q10). Melting and freezing temperatures were observed with a heating rate of 1 K min^{-1} and a cooling rate of 10 K min^{-1}, respectively. Glass transition temperatures were determined as the onset point of the heat signal in the heating cycle with a heating rate of 10 K min^{-1}(see Refs. 6 and 8).

Emulsified samples provide access to measure T_{hom}, since the solution droplets in the emulsions have no contact to surfaces. Emulsions were prepared by adding four parts by weight of a mixture with a lanolin (Fluka Chemical) weight fraction of 0.23 and a mineral oil (Aldrich Chemical) weight fraction of 0.77 to one part of the solution of interest.[36] Stirring with a rotor-stator homogenizer (Polytron PT 1300 D with a PT-DA 1307/2EC dispersing aggregate) for 40 s at 7000 rpm leads to droplets with diameters in the range of 0.5 μm to 5 μm.[37]

Most T_{g} experiments were investigated in bulk samples with masses of roughly 10 to 30 mg. A few T_{g} experiments have also been performed in emulsions to suppress possible heterogeneous ice nucleation prior to glass formation. Zobrist *et al.*[8] showed that emulsified and bulk samples exhibit the same T_{g}.

The solutions were made with distilled and deionized water (resistivity $\geq$18.2 M Ω cm). All substances were used without further purification: raffinose (Sigma, 98%), malonic acid (Fluka, 99%), NH_4HSO_4 (Aldrich, 99.999%),

TABLE I. Measured T_g's and $c_i^l - c_i^g$'s compared to the range of values found in the literature. All T_g's correspond to the heating onset values. Values are given in [K] and [J K^{-1} mol^{-1}], respectively.

	T_g (this study)	$c_i^l - c_i^g$ (this study)	T_g(lit.)	$c_i^l - c_i^g$(lit.)	Refs.
Glycerol	191.7	87.6	180–190	78–90	40–43
$Ca(NO_3)_2 \cdot 4H_2O$[a]	214.1	40.5	217	36-39	44, 45
Salol	221.2	140.8	215-220	110–118	40, 42, 46–48
o-terphenyl	248.2	135.1	241–249	110-116	40, 42, 46, 49–52
Glucose	293.2	134.4	279–311	126-158	8, 43, 53–59
Probucol	300.5	168.5	295–301	140	51, 60, 61
Phenolphtalein	368.3	171.5	362–363	146	45, 62
Raffinose	377.9	285.1	376–382	278	63–67
Citric acid	281.9	183.7	280–286	160-161	68–71

[a]It is assumed that $Ca(NO_3)_2 \cdot 4H_2O$ loses its crystal water and dissociates into Ca^{2+} and NO_3^- when dissolved in water.

citric acid (Sigma, 99%), and $Ca(NO_3)_2$ (Sigma, 99%). The estimated error in the solution preparation is ±0.005 in weight fraction.

The uncertainty in absolute temperature is ±1.2 K for T_{hom}, ±0.8 K for T_m, and ±0.9 K for T_g, respectively.

The difference in the heat capacities of the liquid and the glass phase of the aqueous solutions and pure substances, $c^l - c^g$ and $c_i^l - c_i^g$, were measured for all investigated bulk samples at T_g in units of J K^{-1} mol^{-1} where it is assumed that the salts dissociate into their ions. The heat capacity calibration was performed using benzoic acid according to the calibration procedure described by Della Gatta *et al.*[38] The uncertainty in $c^l - c^g$ for the investigated aqueous solutions in this study was estimated to be on the order of ±5 J K^{-1} mol^{-1}. Note that the spread in the values of heat capacity difference of pure components, $c_i^l - c_i^g$, found in the literature is large,[34,39] depending on the applied evaluation procedure. Table I compares a number of T_g's and $c_i^l - c_i^g$'s of pure substances measured in this study to the range of values found in the literature. While except for glucose where the literature data are divergent, the observed T_g's are in good agreement with literature values, the deviations for $c_i^l - c_i^g$ can be as high as 30 J K^{-1} mol^{-1}.

IV. RESULTS AND DISCUSSION

This section is divided into two parts. The first part deals with T_g, T_{hom}, and T_m of binary aqueous solutions using citric acid, malonic acid, $Ca(NO_3)_2$, and NH_4HSO_4 as solutes and discusses T_g of pure raffinose. The second part shows experimentally determined glass transition temperatures of multicomponent solutions, which are compared to T_g predictions using different mixing rules and discusses discontinuities in the excess mixing entropies. The mixing rules are based on the data of the binary solutions. Table II lists all values experimentally determined in aqueous solutions.

A. Binary solutions

Figure 1 illustrates the above mentioned competition between crystallization, i.e., homogeneous ice freezing in this case, and glass formation for the aqueous citric acid system.

Under ambient pressure, pure liquid water is metastable below 273.15 K and micrometer sized droplets can be supercooled down to 235 K before ice is formed by homogeneous nucleation.[74–76] Hyperquenching small water samples with cooling rates of the order of 10^5 K s^{-1} prevents ice formation and leads to a vitrification of water at 136 K.[77–79] Albeit this number is still a subject of controversial discussions,[6,80,81] we used this value as T_g of pure water (i.e., $T_{g,1} = 136$ K in Eq. (8), as water is always considered the solvent and component 1 in this study).

In general, a dissolved solute in an aqueous solution increases T_g with respect to the glass transition temperature of pure water. The T_g data points for the aqueous citric acid solutions of this study match the literature data from Maltini *et al.*[68] and Lu and Zografi.[69] The T_g of pure citric acid was experimentally detected at 281.9 K, with a $c_i^l - c_i^g$ of 183.7 J K^{-1} mol^{-1}. The T_g-curve shown in Fig. 1 was calculated using Eq. (8) with $n = 2$, leading to $T_{g,2}$ and k_2 values of 280.1 K and 3.18, respectively. The homogeneous ice freezing and ice melting temperatures of the emulsified samples are also consistent with previous studies (see Refs. 9 and 68).

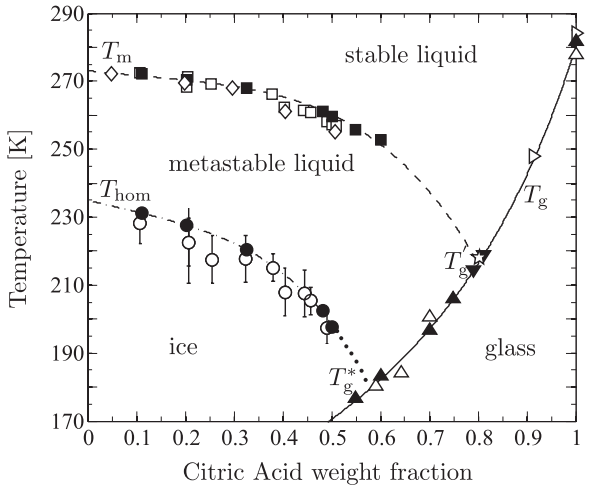

FIG. 1. State diagram of the citric acid-water system as a function of the citric acid weight fraction. The filled symbols are measured points from this study: ■ T_m, ● T_{hom}, ▲ T_g, and ▼ T'_g. Open symbols are from literature: □ T_m and ○ T_{hom} from Murray,[9] ◇ T_m and △ T_g from Maltini *et al.*,[68] ▷ T_g from Lu and Zografi,[69] ★ T'_g from Kadoya *et al.*[72] and Izutsu *et al.*[73] If not explicitly indicated in the plot, the errorbars are within the symbol size.

TABLE II. Measured T_g, T_{hom}, T_g', T_m, and $c^l - c^g$ of the solutions with the indicated weight fraction of the solute, w_2 and w_{tot}, respectively. The solute to solute weight fraction ratios are given in brackets. $c^l - c^g$ of emulsified samples are indicated by "emul" since their value could not be determined. The NH_4HSO_4-data (**B5**) are taken from Zobrist *et al.*[8] and is not listed here. All temperatures are given in [K], the values of $c^l - c^g$ in [J K^{-1} mol^{-1}].

B1: Citric acid						**B2**: $Ca(NO_3)_2$		
w_2	T_g	T_{hom}	T_g'	T_m	$c^l - c^g$	w_2	T_g	$c^l - c^g$
0.111		231.3		272.1	emul	0.476	173.9	33.2
0.204		227.6	214.3	270.3	emul	0.550	184.4	37.2
0.325		220.4		267.9	emul	0.550	185.5	32.2
0.483		201.4		261.0	emul	0.600	193.5	38.9
0.501		197.7	218.8	259.7	emul	0.600	194.6	33.2
0.550	176.6			255.8	emul	0.651	204.2	39.3
0.601	183.3			252.1	41.4	0.695	214.1	40.5
0.702	196.8				61.5			
0.750	206.1				68.7			
1.000	281.9				183.7			

B3: Malonic acid			**B4**: Raffinose			**M1**: Raffinose and NH_4HSO_4 (1:1)		
w_2	T_g	$c^l - c^g$	w_2	T_g	$c^l - c^g$	w_{tot}	T_g	$c^l - c^g$
0.565	165.4	emul	0.607	191.3[a]	34.0	0.502	151.6	emul
0.599	168.9	emul	0.704	219.7[a]	48.0	0.606	163.2	28.5
0.649	172.3	emul	0.772	234.8[a]	48.9	0.689	174.0	35.9
0.700	170.4	emul	0.849	269.6[a]	69.1	0.750	179.6	49.7
0.700	172.4	emul	1.000	377.9	285.1	0.798	185.9	56.1
0.750	172.1	emul				0.851	196.0	57.9

M2: Raffinose and NH_4HSO_4 (3:1)			**M3**: Raffinose and NH_4HSO_4 (6:1)			**M4**: $Ca(NO_3)_2$ and Malonic acid (1:1)		
w_{tot}	T_g	$c^l - c^g$	w_{tot}	T_g	$c^l - c^g$	w_{tot}	T_g	$c^l - c^g$
0.602	171.1	33.4	0.600	178.2	35.7	0.499	170.6	emul
0.655	178.0	41.7	0.700	194.5	49.6	0.499	171.0	39.8
0.712	190.6	52.5	0.800	221.3	61.2	0.600	181.9	48.9
0.749	199.8	54.7	0.851	238.9	71.4	0.700	198.4	51.9
0.800	210.5	57.1				0.750	207.4	59.6
0.850	225.7	62.9				0.800	218.7	60.7

M5: $Ca(NO_3)_2$ and Raffinose (1:1)			**M6**: Citric acid, Raffinose and NH_4HSO_4 (1:1:1)		
w_{tot}	T_g	$c^l - c^g$	w_{tot}	T_g	$c^l - c^g$
0.550	175.8	36.0	0.550	158.5	26.9
0.600	185.2	41.3	0.607	166.3	32.9
0.699	203.1	48.6	0.699	180.0	47.2
0.764	237.5	44.5	0.750	191.0	55.9
			0.795	196.5	63.6

[a]Values taken from Zobrist *et al.*[8]

The sparse scattering in our T_{hom}-data highlights the quality and consistency of the emulsion technique investigated in a DSC.

T_g' is the so-called glass transition temperature of the freeze-concentrated solution and can be experimentally determined in the DSC (Ref. 82). When ice freezing takes place before glass formation, the remaining liquid part of the sample gets more concentrated with respect to the solute. Further cooling leads to vitrification of the remaining solution at T_g' (see Refs. 8, 72, and 73). T_g' itself depends on the experimental procedure,[8,53] which can lead to strong deviations in T_g' between different studies. In our experiments, values of 214.3 K and 218.8 K were obtained for two different concentrations, exhibiting close agreement with the values given by Kadoya *et al.*[72] and Izutsu *et al.*[73]

The T_m- and T_{hom}-curves in Fig. 1 (dashed and dash-dotted lines) are fit functions of the form of a fourth degree polynomial, omitting the third degree. This function has been chosen because it is the simplest function that shows good agreement with the measured points. The T_m-curve was constrained such that it fits through the T_g' of 216.6 K, the mean value of the two experimentally determined T_g' in this study. The function of the T_m-curve is $T_m = 273.15 - 15.18w_2 + 9.641(w_2)^2 - 123.7(w_2)^4$ for $w_2 \leq 0.800$.

TABLE III. Glass transition temperatures $T_{g,2}$ of the pure solutes (**B1**–**B5**) applied in this study and their respective k_2, both calculated using Eq. (8). The uncertainties $\sigma(T_{g,2})$ and $\sigma(k_2)$ define the 95% confidence bounds of $T_{g,2}$ and k_2, respectively. The aqueous multi-component systems **M1**–**M6** contain the indicated solutes with the specified solute to solute weight fraction ratio indicated in brackets. The symbols correspond to the ones used in Figs. 2–4. RMSE denotes the root mean square error defined by Eq. (11) for m measurements. The subscripts C and Z stand for the approaches by Couchman and Karasz[28] and Zobrist *et al.*,[8] respectively, for which the RMSE's were calculated separately. The values for **B5** are taken from Zobrist *et al.*[8] All other values listed here are based on the data presented in Table II and on experimental data found in the literature for citric acid (Refs. 68–71), $Ca(NO_3)_2$ (Refs. 44, 45, 83, and 84), and Raffinose Refs. 8 and 63–66.

Solutes (bin.)		$T_{g,2}$	$\sigma(T_{g,2})$	k_2	$\sigma(k_2)$	RMSE	m	Solutes (mult.)		$RMSE_C$	$RMSE_Z$	m
B1: Citric acid	△	280.1	3.7	3.18	0.24	2.24	9	**M1**: Raffinose and NH_4HSO_4 (1:1)	●	7.5	5.1	6
B2: $Ca(NO_3)_2$	▽	387.4	24.1	5.04	0.62	0.80	19	**M2**: Raffinose and NH_4HSO_4 (3:1)	■	7.0	9.4	6
B3: Malonic Acid	▷	179.4	11.3	0.52	0.63	1.72	6	**M3**: Raffinose and NH_4HSO_4 (6:1)	♦	6.3	7.7	4
B4: Raffinose	◯	378.3	8.7	4.76	0.42	2.95	6	**M4**: $Ca(NO_3)_2$ and Malonic acid (1:1)	►	22.7	11.4	4
B5: NH_4HSO_4	□	178.0	13.9	1.55	1.28	1.43	5	**M5**: $Ca(NO_3)_2$ and Raffinose (1:1)	◄	8.4	9.0	4
								M6: Citric acid, raffinose and NH_4HSO_4 (1:1:1)	▲	7.4	4.7	5

T_g^* denotes the intersection between the glass transition and the homogeneous ice freezing curves, which has no experimental access. At lower concentrations, ice formation is more likely when using moderate cooling rates. At higher concentrations, however, the sample vitrifies. For the T_{hom}-curve, the best fit curve is $T_{hom} = 235 - 34.45w_2 + 3.996(w_2)^2 - 324.3(w_2)^4$, for $w_2 \leq 0.501$. The dotted line represents the extrapolation of the T_{hom}-curve where no data are available. The dotted line crosses the T_g-curve at $T_g^* = 179.6$ K, which corresponds to a citric acid weight fraction of 0.580. Murray[9] recently obtained a value of 180 K.

One citric acid experiment with a weight fraction of 0.550 was performed in an emulsified sample since heterogeneous ice freezing occurred on the pan surface when a bulk sample was used. Ice nucleation could have occurred in the emulsified sample, but ice growth was possibly inhibited due to the large viscosity. However, the DSC-technique is only sensitive to the ice growth but not the ice nucleation. On the other hand, crystallization was observed upon heating above T_g which confirms the formation of ice germs in the cooling cycle that trigger ice growth in the heating cycle while still in the metastable range. This crystallization allowed us to measure both T_g and T_m for this sample.

The other binary systems investigated in this study were aqueous $Ca(NO_3)_2$ and aqueous malonic acid. The T_g-values of aqueous $Ca(NO_3)_2$ samples are in close agreement with values found by Angell *et al.*[83] and Pedernera[84] at similar concentrations. T_g of solutions with $Ca(NO_3)_2$-weight fractions larger than 0.695 could not be investigated because of the formation of crystals, probably $Ca(NO_3)_2 \cdot 4H_2O$, the most stable hydrate.

All experiments with aqueous malonic acid solutions were performed in emulsions. Glass transitions were observed only between weight fractions of 0.565 and 0.750. At lower and higher concentrations ice and solid malonic acid (probably in the form of malonic acid hexahydrate[85]), respectively, formed during the experiments. The sample with a malonic acid weight fraction of 0.750 showed a glass transition at 172.1 K and then was heated up to temperatures above the melting point of pure malonic acid (407.46 K (Ref. 85)), but no melting signal was found in the DSC-thermograms. This indicates the absence of malonic acid crystallization during the experiment that would have adversely affected the observed value of T_g.

Raffinose was supplied as pentahydrate. It was dried at 470 K for two days in an oven, leading to an anhydrous raffinose. The sample was weighed before and after the drying. The difference in mass matched the expected amount of crystal water initially present in the pentahydrate. Glass formation in such a sample with pure raffinose occurred at 377.9 K, which is in good agreement with literature values (see Table I). This value is also roughly 15 K smaller than the computed value by Zobrist *et al.*,[8] but still agrees within the uncertainty range of their extrapolation.

Table III summarizes the calculated $T_{g,2}$ and k_2 of the solutes in the binary systems investigated in this study (**B1**–**B5**), which will be used later to model the multi-component systems.

B. Multi-component systems

The Couchman–Karasz equation computes T_g of a multi-component mixture when the k_i's and $T_{g,i}$'s are known for the included binary systems.

Six multi-component mixtures (**M1**–**M6**) have been investigated in total that were made of water as solvent and the five substances discussed in Sec. IV A as solutes. Table III lists the investigated solutions with their respective solute to solute weight fraction ratios. w_{tot} denotes the sum of the weight fractions of each solute. Figure 2 shows the experimental glass transition temperatures for the multi-component solutions together with predicted T_g-curves as well as the binary glass transition curves. The solid lines represent the predicted T_g-curves of the multi-component systems according to the Couchman–Karasz equation. The dashed lines display the corresponding binary curves in each plot.

Alternatively to the Couchman–Karasz equation, Zobrist *et al.*[8] proposed an empirical mixing rule based on the glass transition temperatures of a few multi-component solutions. This mixing rule also predicts T_g of a multi-component system depending on k_i and $T_{g,i}$ of the involved solutes,

$$T_g = \frac{\sum_{i=2} \frac{w_i}{M_i} T_{g,i}(w_{tot})}{\sum_{i=2} \frac{w_i}{M_i}}. \quad (10)$$

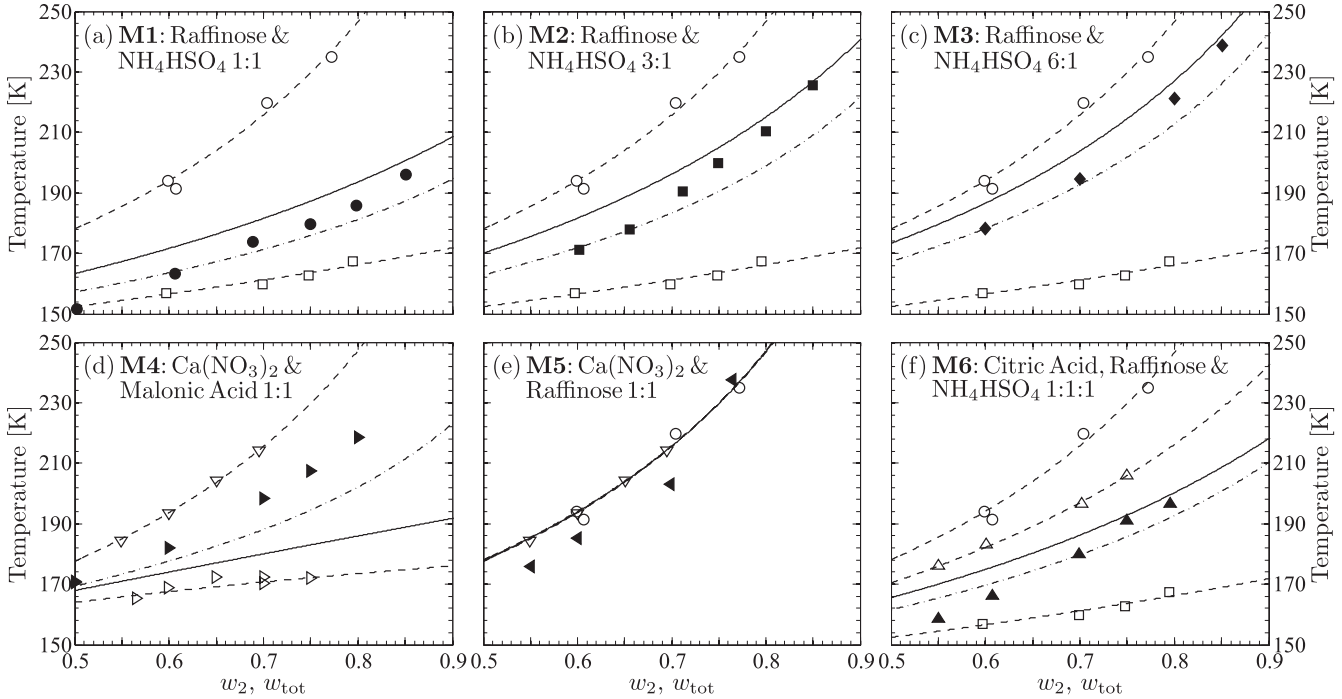

FIG. 2. T_g of binary and multi-component aqueous solutions versus solute weight fraction, w_2 and w_{tot}, respectively. Symbols and abbreviations are as described in Table III. The dashed lines show the glass transition curves of the binary solutions, the solid lines the prediction for the multi-component system by the Couchman–Karasz equation (Eq. (8)), and the dash-dotted lines the prediction by the empirical mixing rule proposed by Zobrist *et al.*[8] (Eq. (10)). All experimental uncertainties of the glass transition temperatures are within the symbol size.

In this approach, T_g is calculated as the sum of the T_g's of the binary mixtures computed with the Couchman–Karasz equation but using w_{tot} instead of w_i for each binary contribution, weighted by their respective mole fraction. Equation (10) and the Couchman–Karasz equation coincide for binary solutions. In Fig. 2, the predictions of Eq. (10) are represented by the dash-dotted lines.

Panels (a)–(c) show T_g of aqueous NH_4HSO_4 and raffinose mixtures, with a raffinose to NH_4HSO_4 weight fraction ratio varying from 1:1, to 3:1 up to 6:1. T_g-curves calculated with the Couchman–Karasz equation constantly overestimate the experimental data. The curves predicted by Eq. (10) underestimate the data at higher concentrations, but show better agreement at lower concentrations. Panel (d) displays the system with malonic acid and $Ca(NO_3)_2$ as solutes with equal weight fraction ratios. The data points are closer to the T_g-curve of $Ca(NO_3)_2$ and both fit approaches clearly underestimate the experimental data, with higher deviations observed for the Couchman–Karasz equation. The solutes applied in panel (e), raffinose and $Ca(NO_3)_2$, exhibit almost equal binary T_g-curves and thus, both binary fit curves coincide. This example provides evidence for both negative and positive deviation from either fit curve in a solution with three components. Panel (f) shows the measured T_g for solutions consisting of three solutes: raffinose, NH_4HSO_4, and citric acid with equal weight fractions. The position of the data points with respect to the two fit curves are similar to the ternary raffinose/NH_4HSO_4-solutions shown in panels (a)–(c).

The measured T_g's in all investigated multi-component solutions exhibit large deviations from their predicted T_g with values up to 31.8 K (mixture **M4**, mass fraction of solute of 0.800). The accuracy of the predictions is clearly lower than the accuracy of the fit of the binary systems. In order to quantify the discrepancy between the measured and the predicted T_g's, the root mean square errors (RMSE's) are calculated in Table III for both binary and multi-component solutions,

$$\mathrm{RMSE} = \sqrt{\frac{\sum_p^m \left(x_p^{fit} - x_p^{ex}\right)^2}{m}}, \tag{11}$$

where m is the total number of measured T_g's for the solute in consideration, x_p^{fit} the computed and x_p^{ex} the experimentally determined T_g of the p^{th} measurement. Binary systems exhibit small RMSE, complex mixtures higher RMSE (see $\mathrm{RMSE_C}$ for Eq. (8) and $\mathrm{RMSE_Z}$ for Eq. (10) in Table III). In general, the empirical equation by Zobrist *et al.*[8] performs as good as the Couchman–Karasz equation, but both show significant deviations from the measurements.

The differences between the mixing rules and the experimental data in the multi-component solutions might result from the term $(\Delta S^l_{mix} - \Delta S^g_{mix})$ exhibiting non-zero values at the respective glass transition with the chosen values of the k_i's. As a consequence, the approximation from Eq. (5) to Eq. (8) can no longer be applied. In other terms, the molecular interactions in the liquid state differ from those interactions in the glassy state at the glass transition temperature. Goldstein[86] already questioned whether the term $(\Delta S^l_{mix} - \Delta S^g_{mix})$ can be neglected in Eq. (5) as suggested by Couchman and Karasz.[28] The entropy contributions due to non-configurational mixing could alter abruptly as the sample vitrifies, which would clearly affect T_g (Refs. 86–89). Albeit this effect might be small in many compatible polymer systems, it could change

T_g in multi-component mixtures as shown here considerably. In a different approach, Pinal[33] interprets the deviation from the Couchman–Karasz equation as "a result of the liquid-accessible configurational entropy of mixing," which is the part of the configurational entropy that gets consumed upon cooling until glass transition occurs.

To find $\Delta S^{l}_{mix} - \Delta S^{g}_{mix}$ of the investigated solutions, we rearrange Eq. (5) into

$$\Delta S^{l}_{mix} - \Delta S^{g}_{mix} = \frac{w_1(T_{g,1} - T_g) + \sum_{i=2}^{n} w_i \frac{1}{k_i}(T_{g,i} - T_g)}{T_g \frac{1}{c_1^l - c_1^g}\left(w_1 + \sum_{i=2}^{n} w_i \frac{M_1}{M_i}\right)}. \quad (12)$$

Thus, one could find $\Delta S^{l}_{mix} - \Delta S^{g}_{mix}$ provided that $c_1^l - c_1^g$ and $c_i^l - c_i^g$ are known and temperature independent. $c_1^l - c_1^g$ is still subject to debate.[90] While hyperquenching experiments[79,91,92] show a $c_1^l - c_1^g$ of 0.7–2 J K^{-1} mol^{-1}, extrapolations from dilute aqueous solutions containing salts investigated by Angell and Tucker[93] suggest a value around 21 J K^{-1} mol^{-1} at 136 K. Oguni and Angell[94] and more recently Corti *et al.*[95] found a value of 35 J K^{-1} mol^{-1} for $c_1^l - c_1^g$ from binary aqueous solutions containing hydrazine (N_2H_4), hydrogen peroxide (H_2O_2), and phosphorus pentoxide (P_2O_5), respectively. These discrepancies are explained in terms of a "fragile-to-strong" liquid transition of very dilute solutions which is experimentally inaccessible due to homogeneous ice freezing.[82,95] This transition and hence the $c_1^l - c_1^g$ which should be used in Eq. (6) depend on the solute. Corti *et al.*[82] recommend 35 J K^{-1} mol^{-1} for fragile molecular solutions and a lower value for salt containing solutions.

Since most of the solutions investigated in this study contain salts, $c_1^l - c_1^g$ is evaluated for each mixture individually. Similar to the procedure described by Corti *et al.*,[95] we plot the $c^l - c^g$'s as a function of mole fraction of water in Fig. 3. The data are split into three panels for reasons of clarity. The values of $c_1^l - c_1^g$ for each mixture can be found by extrapolating the linear concentration dependence of $c^l - c^g$ to pure water. These linear fits yield a rough estimate of $c_1^l - c_1^g$ since the number of measured points is very limited and the concentration dependence could deviate from linear behavior over the concentration range shown.

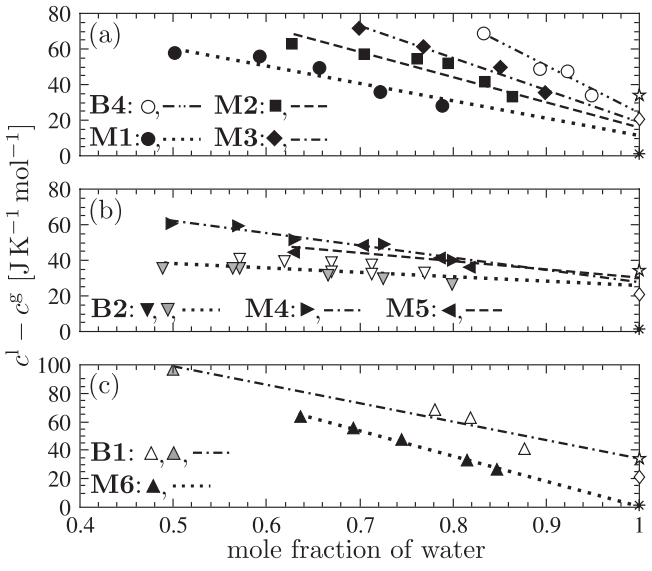

FIG. 3. $c^l - c^g$ of the investigated bulk aqueous solutions as a function of mole fraction of water. The symbols correspond to the ones introduced in Table III together with literature data of citric acid gray filled △ (Ref. 69) and $Ca(NO_3)_2$ gray filled ▽ (Refs. 44 and 93). The lines show the linear concentration dependences of $c^l - c^g$. Additionally, the proposed $c_1^l - c_1^g$ of 0.7–2 J K^{-1} mol^{-1} (*), 21 J K^{-1} mol^{-1} (◇), and 35 J K^{-1} mol^{-1} (★) are also indicated (see Refs. 79, 82, and 91–95). The uncertainty in $c^l - c^g$ is estimated to be ±5 J K^{-1} mol^{-1}.

Panel (a) shows that $c_1^l - c_1^g$ in raffinose/NH_4HSO_4 containing solutions increases with decreasing salt concentration. The fitted values for $c_1^l - c_1^g$ of 12 J K^{-1} mol^{-1} for **M1**, 17 J K^{-1} mol^{-1} for **M2**, 19 J K^{-1} mol^{-1} for **M3**, and 25 J K^{-1} mol^{-1} for binary raffinose solutions, are lower than expected. In panel (b), the $c_1^l - c_1^g$ estimated for binary $Ca(NO_3)_2$ solutions of 26 J K^{-1} mol^{-1} is close to solutions where malonic acid or raffinose are added as third components, exhibiting values of 28 J K^{-1} mol^{-1} (**M4**) and 30 J K^{-1} mol^{-1} (**M5**), respectively. The extrapolation for citric acid, shown in panel (c), yields 34 J K^{-1} mol^{-1} for $c_1^l - c_1^g$, in agreement with binary P_2O_5, H_2O_2, and N_2H_4 solutions.[94,95] Mixture **M6** which also contains citric acid seems to behave differently than the other systems investigated in this study. The linear fit approaches negative values, which is unphysical. This inconsistency might be due to nonlinear behavior in the experimentally inaccessible concentration range.

These estimates can now be used to calculate k_2^{cal} according to Eq. (6). For citric acid, this results in 1.98 with our $c_i^l - c_i^g$ and 2.27 if $c_i^l - c_i^g$ reported by Lu and Zografi[69] and Hoppu *et al.*[71] are used. Both values are considerably lower than the fitted k_2 of 3.18. $c_1^l - c_1^g$ would need to be between 48 and 55 J K^{-1} mol^{-1} to bring the fitted and the calculated value into agreement.

For raffinose, k_2^{cal} is 2.46 if 25 J K^{-1} mol^{-1} are applied for $c_1^l - c_1^g$ and 3.44 if 35 J K^{-1} mol^{-1} are used. In this case, 48 J K^{-1} mol^{-1} for $c_1^l - c_1^g$ would be needed to bring k_2 and k_2^{cal} into agreement. Based on the data shown in Fig. 3, it is unlikely that $c_1^l - c_1^g$ reaches such high values.

For the aqueous citric acid and raffinose solutions, the computed k_2^{cal} can be inserted in Eq. (12) together with the T_g's calculated with the fitted k_2's to yield a function of $\Delta S^{l}_{mix} - \Delta S^{g}_{mix}$ over all concentrations, represented by the dashed and dotted lines in panel (a) of Fig. 4. (Ref. 33). The discontinuity of the excess mixing entropy in these mixtures where the fitted k_2's well represent the measured points suggests that the fitted k_2's take these discontinuities into account.

For some substances of the multi-component systems, the k_2^{cal}'s could not be evaluated since $c_i^l - c_i^g$ are experimentally inaccessible. Thus, the fitted k_2's were inserted in Eq. (12) as k_i's together with the measured T_g's of the multi-component systems which only gives values for the measured concentrations. In this case, the resulting quantity represents that part of the excess mixing discontinuity that is not represented by using the fitted k_2's from the binary mixtures. Thus, this quantity is called $\Delta S^{l}_{mix} - \Delta S^{g}_{mix}$(mult) and is shown in two different panels (b) and (c) of Fig. 4 for reasons of clarity.

Since all points in Fig. 4 depend on $c_1^l - c_1^g$, their uncertainties are large. Nevertheless it follows from Eq. (12) that $c_1^l - c_1^g$ only scales the values of $\Delta S^{l}_{mix} - \Delta S^{g}_{mix}$ and

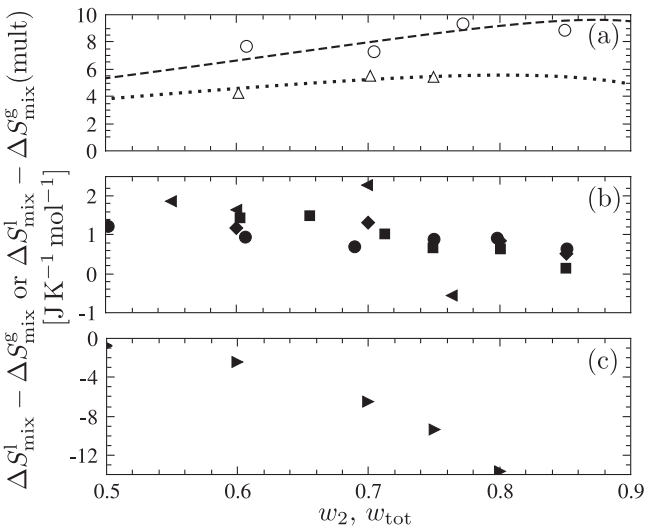

FIG. 4. $\Delta S^{l}_{mix} - \Delta S^{g}_{mix}$ and $\Delta S^{l}_{mix} - \Delta S^{g}_{mix}$(mult) of (a) citric acid (**B1**) and raffinose (**B4**), (b) **M1**, **M2**, **M3**, and **M5**, and (c) **M4** versus solute weight fraction, w_2 and w_{tot}, respectively. The symbols correspond to the symbols introduced in Table III. The lines in panel (a) represent the calculated $\Delta S^{l}_{mix} - \Delta S^{g}_{mix}$ for citric acid (dotted line) and raffinose (dashed line).

$\Delta S^{l}_{mix} - \Delta S^{g}_{mix}$(mult) on the y axis, but does not change the relative quantities in each system.

The $\Delta S^{l}_{mix} - \Delta S^{g}_{mix}$(mult) displayed in panel (b) for the mixtures **M1**, **M2**, **M3**, and **M5** are smaller than the ones of the binary mixtures. In general, the values seem to decrease towards $w_{tot} = 1$, in agreement with the small deviation between the experimentally observed and the computed T_g at higher w_{tot}. $\Delta S^{l}_{mix} - \Delta S^{g}_{mix}$(mult) might not be zero at $w_{tot} = 1$ as there are still two species present in the mixture. As the interactions in the liquid state are generally expected to be larger than interactions in the glassy state, most values are positive, i.e., $\Delta S^{l}_{mix} > \Delta S^{g}_{mix}$.

System **M4** in panel (c) exhibits high negative values of $\Delta S^{l}_{mix} - \Delta S^{g}_{mix}$(mult). This result could arise from differences in the interactions between water and the solutes for the binary solutions compared to the ternary mixtures. The fitted k_2's of malonic acid and $Ca(NO_3)_2$ do not take this difference into account.

V. CONCLUSIONS

Differential scanning calorimetry was used to investigate the glass transition temperatures of aqueous solutions containing citric acid, raffinose, NH_4HSO_4, $Ca(NO_3)_2$, and malonic acid. The results presented in Figs. 1 and 2 suggest a good agreement with the fitted Couchman–Karasz equation for binary mixtures.

The complex multi-component solutions investigated in this study exhibit significant deviations from their predicted T_g based on the k_2's of the binary systems, which implies that the excess mixing entropy of the liquid ΔS^{l}_{mix} and the excess mixing entropy of the glass ΔS^{g}_{mix} at T_g are not equal.

The mismatch between the fitted k_2's and the computed k_2^{cal}'s derived from the differences in the heat capacities suggests that $\Delta S^{l}_{mix} - \Delta S^{g}_{mix}$ also exhibits non-zero values in binary mixtures. However, the fitted k_2's account for discontinuities of the excess mixing entropies.

Glass transitions in atmospheric aerosols are hardly predictable due to the myriad of components. We find that even if the k_2's of all components are known, the quantity $\Delta S^{l}_{mix} - \Delta S^{g}_{mix}$(mult) would lead to a deviation between the predicted and the observed T_g. The mixing rules proposed by Couchman and Karasz[28] and the empirical equation by Zobrist *et al.*[8] should therefore be considered an estimation rather than an accurate prediction.

ACKNOWLEDGMENTS

This research was supported by the European Commission through the EC Integrated Projects SCOUT-O3 (505390-GOCE-CT-2004) and the ETH Research Grant ETH-0210-1.

[1] P. G. Debenedetti and F. H. Stillinger, Nature (London) **410**, 259 (2001).
[2] M. C. Boyce, D. M. Parks, and A. S. Argon, Mech. Mater. **7**, 15 (1988).
[3] R. Franke, B. Maennig, A. Petrich, and M. Pfeiffer, Sol. Energy Mater. Sol. Cells **92**, 732 (2008).
[4] L. Slade and H. Levine, J. Food Eng. **22**, 143 (1994).
[5] B. C. Hancock, S. L. Shamblin, and G. Zografi, Pharm. Res. **12**, 799 (1995).
[6] C. A. Angell, Chem. Rev. **102**, 2627 (2002).
[7] P. Jenniskens and D. F. Blake, Science **265**, 753 (1994).
[8] B. Zobrist, C. Marcolli, D. A. Pedernera, and T. Koop, Atmos. Chem. Phys. **8**, 5221 (2008).
[9] B. J. Murray, Atmos. Chem. Phys. **8**, 5423 (2008).
[10] B. Graham, O. L. Mayol-Bracero, P. Guyon, G. C. Roberts, S. Decesari, M. C. Facchini, P. Artaxo, W. Maenhaut, P. Koll, and M. O. Andreae, J. Geophys. Res. **107**, 8047, doi:10.1029/2001JD000336 (2002).
[11] S. Decesari, S. Fuzzi, M. C. Facchini, M. Mircea, L. Emblico, F. Cavalli, W. Maenhaut, X. Chi, G. Schkolnik, A. Falkovich, Y. Rudich, M. Claeys, V. Pashynska, G. Vas, I. Kourtchev, R. Vermeylen, A. Hoffer, M. O. Andreae, E. Tagliavini, F. Moretti, and P. Artaxo, Atmos. Chem. Phys. **6**, 375 (2006).
[12] M. Kanakidou, J. H. Seinfeld, S. N. Pandis, I. Barnes, F. J. Dentener, M. C. Facchini, R. Van Dingenen, B. Ervens, A. Nenes, C. J. Nielsen, E. Swietlicki, J. P. Putaud, Y. Balkanski, S. Fuzzi, J. Horth, G. K. Moortgat, R. Winterhalter, C. E. L. Myhre, K. Tsigaridis, E. Vignati, E. G. Stephanou, and J. Wilson, Atmos. Chem. Phys. **5**, 1053 (2005).
[13] D. M. Murphy, D. J. Cziczo, K. D. Froyd, P. K. Hudson, B. M. Matthew, A. M. Middlebrook, R. E. Peltier, A. Sullivan, D. S. Thomson, and R. J. Weber, J. Geophys. Res. **111**, D23S32, doi:10.1029/2006JD007340 (2006).
[14] K. D. Froyd, D. M. Murphy, T. J. Sanford, D. S. Thomson, J. C. Wilson, L. Pfister, and L. Lait, Atmos. Chem. Phys. **9**, 4363 (2009).
[15] E. Mikhailov, S. Vlasenko, S. T. Martin, T. Koop, and U. Poeschl, Atmos. Chem. Phys. **9**, 9491 (2009).
[16] B. Zobrist, V. Soonsin, B. P. Luo, U. K. Krieger, C. Marcolli, T. Peter, and T. Koop, Phys. Chem. Chem. Phys. **13**, 3514 (2011).
[17] H.-J. Tong, J. P. Reid, D. L. Bones, B. P. Luo, and U. K. Krieger, Atmos. Chem. Phys. **11**, 4739 (2011).
[18] D. J. Cziczo, P. J. DeMott, S. D. Brooks, A. J. Prenni, D. S. Thomson, D. Baumgardner, J. C. Wilson, S. M. Kreidenweis, and D. M. Murphy, Geophys. Res. Lett. **31**, L12116, doi:10.1029/2004GL019822 (2004).
[19] E. J. Jensen, J. B. Smith, L. Pfister, J. V. Pittman, E. M. Weinstock, D. S. Sayres, R. L. Herman, R. F. Troy, K. Rosenlof, T. L. Thompson, A. M. Fridlind, P. K. Hudson, D. J. Cziczo, A. J. Heymsfield, C. Schmitt, and J. C. Wilson, Atmos. Chem. Phys. **5**, 851 (2005).
[20] P. J. DeMott, M. D. Petters, A. J. Prenni, C. M. Carrico, S. M. Kreidenweis, J. L. Collett, and H. Moosmuller, J. Geophys. Res. **114**, D16205, doi:10.1029/2009JD012036 (2009).
[21] M. Kraemer, C. Schiller, A. Afchine, R. Bauer, I. Gensch, A. Mangold, S. Schlicht, N. Spelten, N. Sitnikov, S. Borrmann, M. de Reus, and P. Spichtinger, Atmos. Chem. Phys. **9**, 3505 (2009).
[22] P. G. Debenedetti, *Metastable Liquids: Concepts and Principles* (Princeton University, Princeton, NJ, 1996).
[23] C. A. Angell, Science **267**, 1924 (1995).

[24]D. M. Murphy and T. Koop, Q. J. R. Meteorol. Soc. **131**, 1539 (2005).
[25]J. H. Gibbs and E. A. DiMarzio, J. Chem. Phys. **28**, 373 (1958).
[26]E. A. DiMarzio and J. H. Gibbs, J. Chem. Phys. **28**, 807 (1958).
[27]G. Adam and J. H. Gibbs, J. Chem. Phys. **43**, 139 (1965).
[28]P. R. Couchman and F. E. Karasz, Macromolecules **11**, 117 (1978).
[29]J. M. Gordon and J. S. Taylor, J. Appl. Chem. **2**, 493 (1952).
[30]C. R. Usher, A. E. Michel, and V. H. Grassian, Chem. Rev. **103**, 4883 (2003).
[31]P. R. Couchman, Macromolecules **11**, 1156 (1978).
[32]P. W. Atkins and J. de Paula, *Physical Chemistry* (Oxford University Press, Oxford, 2010).
[33]R. Pinal, Entropy **10**, 207 (2008).
[34]I. I. Katkov and F. Levine, Cryobiology **49**, 62 (2004).
[35]J. M. Gordon, G. B. Rouse, J. H. Gibbs, and W. M. Risen, J. Chem. Phys. **66**, 4971 (1977).
[36]B. Zobrist, C. Marcolli, T. Koop, B. P. Luo, D. M. Murphy, U. Lohmann, A. A. Zardini, U. K. Krieger, T. Corti, D. J. Cziczo, S. Fueglistaler, P. K. Hudson, D. S. Thomson, and T. Peter, Atmos. Chem. Phys. **6**, 3115 (2006).
[37]C. Marcolli, S. Gedamke, T. Peter, and B. Zobrist, Atmos. Chem. Phys. **7**, 5081 (2007).
[38]G. Della Gatta, M. J. Richardson, S. M. Sarge, and S. Stolen, Pure Appl. Chem. **78**, 1455 (2006).
[39]L. M. Wang, C. A. Angell, and R. Richert, J. Chem. Phys. **125**, 074505 (2006).
[40]L. M. Wang, V. Velikov, and C. A. Angell, J. Chem. Phys. **117**, 10184 (2002).
[41]E. J. Donth, *Relaxation and Thermodynamics in Polymers: Glass Transition* (Akademie Verlag Gmbh, Berlin, 1992).
[42]R. Boehmer, K. L. Ngai, C. A. Angell, and D. J. Plazek, J. Chem. Phys. **99**, 4201 (1993).
[43]G. S. Parks, S. B. Thomas, and W. A. Gilkey, J. Phys. Chem. **34**, 2028 (1930).
[44]C. A. Angell and J. C. Tucker, J. Phys. Chem. **78**, 278 (1974).
[45]J. D. Stevenson and P. G. Wolynes, J. Phys. Chem. B **109**, 15093 (2005), and references therein.
[46]W. T. Laughlin and D. R. Uhlmann, J. Phys. Chem. **76**, 2317 (1972).
[47]T. Hikima, M. Hanaya, and M. Oguni, Solid State Commun. **93**, 713 (1995).
[48]J. K. Krueger, R. Holtwick, A. le Coutre, and J. Baller, Nanostruct. Mater. **12**, 519 (1999).
[49]S. S. Chang and A. B. Bestul, J. Chem. Phys. **56**, 503 (1972).
[50]T. Atake and C. A. Angell, J. Phys. Chem. **83**, 3218 (1979).
[51]K. J. Crowley and G. Zografi, Thermochim. Acta **380**, 79 (2001).
[52]F. Fujara, B. Geil, H. Sillescu, and G. Fleischer, Z. Phys. B: Condens. Matter **88**, 195 (1992).
[53]Y. H. Roos, Carbohydr. Res. **238**, 39 (1993).
[54]H. P. Diogo and J. J. Moura Ramos, Carbohydr. Res. **343**, 2797 (2008).
[55]R. Wungtanagorn and S. J. Schmidt, Thermochim. Acta **369**, 95 (2001).
[56]K. Kawai, T. Hagiwara, R. Takai, and T. Suzuki, Pharm. Res. **22**, 490 (2005).
[57]R. K. Chan, K. Pathmanathan, and G. P. Johari, J. Phys. Chem. **90**, 6358 (1986).
[58]P. D. Orford, R. Parker, and S. G. Ring, Carbohydr. Res. **196**, 11 (1990).
[59]P. D. Orford, R. Parker, S. G. Ring, and A. C. Smith, Int. J. Biol. Macromol. **11**, 91 (1989).
[60]E. Broman, C. Khoo, and L. S. Taylor, Int. J. Pharm. **222**, 139 (2001).
[61]P. Thybo, B. L. Pedersen, L. Hovgaard, R. Holm, and A. Mullertz, Pharm. Dev. Technol. **13**, 375 (2008).
[62]M. Pizzoli, M. Scandola, G. Ceccorulli, and G. Pezzin, Polym. Bull. **9**, 429 (1983).
[63]J. J. Maura Ramos, S. S. Pinto, and H. P. Diogo, Pharm. Res. **22**, 1142 (2005).
[64]J. Buitink, I. J. van den Dries, F. A. Hoekstra, M. Alberda, and M. A. Hemminga, Biophys. J. **79**, 1119 (2000).
[65]K. Kajiwara and F. Franks, J. Chem. Soc., Faraday Trans. **93**, 1779 (1997).
[66]K. Kajiwara, F. Franks, P. Echlin, and A. L. Greer, Pharm. Res. **16**, 1441 (1999).
[67]A. Saleki-Gerhardt, J. G. Stowell, S. R. Byrn, and G. Zografi, J. Pharm. Sci. **84**, 318 (1995).
[68]E. Maltini, M. Anese, and I. Shtylla, CryoLetters **18**, 263 (1997).
[69]Q. Lu and G. Zografi, J. Pharm. Sci. **86**, 1374 (1997).
[70]R. J. Timko and N. G. Lordi, J. Pharm. Sci. **68**, 601 (1979).
[71]P. Hoppu, S. Hietala, S. Schantz, and A. M. Juppo, Eur. J. Pharm. Biopharm. **71**, 55 (2009).
[72]S. Kadoya, K. I. Izutsu, E. Yonemochi, K. Terada, C. Yomota, and T. Kawanishi, Chem. Pharm. Bull. (Tokyo) **56**, 821 (2008).
[73]K. Izutsu, S. Kadoya, C. Yomota, T. Kawanishi, E. Yonemochi, and K. Terada, Chem. Pharm. Bull. (Tokyo) **57**, 43 (2009),
[74]H. Kanno, R. J. Speedy, and C. A. Angell, Science **189**, 880 (1975).
[75]T. Koop, B. P. Luo, A. Tsias, and T. Peter, Nature (London) **406**, 611 (2000).
[76]M. B. Baker and M. Baker, Geophys. Res. Lett. **31**, L19102, doi:10.1029/2004GL020483 (2004).
[77]E. Mayer, J. Appl. Phys. **58**, 663 (1985).
[78]G. P. Johari, A. Hallbrucker, and E. Mayer, Nature (London) **330**, 552 (1987).
[79]I. Kohl, L. Bachmann, A. Hallbrucker, E. Mayer, and T. Loerting, Phys. Chem. Chem. Phys. **7**, 3210 (2005).
[80]Y. Z. Yue and C. A. Angell, Nature (London) **427**, 717 (2004).
[81]G. P. Johari, J. Chem. Phys. **116**, 8067 (2002).
[82]H. R. Corti, C. A. Angell, T. Auffret, H. Levine, M. Pilar Buera, D. S. Reid, Y. H. Roos, and L. Slade, Pure Appl. Chem. **82**, 1065 (2010).
[83]C. A. Angell, E. J. Sare, J. Donnella, and D. R. MacFarlane, J. Phys. Chem. **85**, 1461 (1981).
[84]D. A. Pedernera, *Glasbildung in Aerosolpartikeln der oberen Troposphaere*, Ph.D. dissertation, (University of Bielefeld, 2008).
[85]A. R. Hansen and K. D. Beyer, J. Phys. Chem. A **108**, 3457 (2004).
[86]M. Goldstein, Macromolecules **18**, 277 (1985).
[87]M. Goldstein, J. Chem. Phys. **64**, 4767 (1976).
[88]M. Goldstein, J. Chem. Phys. **67**, 2246 (1977).
[89]R. J. Roe and A. E. Tonelli, Macromolecules **11**, 114 (1978).
[90]C. A. Angell, Science **319**, 582 (2008).
[91]A. Hallbrucker, E. Mayer, and G. P. Johari, J. Phys. Chem. **93**, 4986 (1989).
[92]G. P. Johari, G. Fleissner, A. Hallbrucker, and E. Mayer, J. Phys. Chem. **98**, 4719 (1994).
[93]C. A. Angell and J. C. Tucker, J. Phys. Chem. **84**, 268 (1980).
[94]M. Oguni and C. A. Angell, J. Chem. Phys. **73**, 1948 (1980).
[95]H. R. Corti, F. J. Nores-Pondal, and C. A. Angell, Phys. Chem. Chem. Phys. **13**, 19741 (2011).